Research paper

Clocking divergence of iterative maps of matrices

Rasa Smidtaite [a,b], Zenonas Navickas [a], Minvydas Ragulskis [a,*]

[a] Center for Nonlinear Systems, Kaunas University of Technology, Studentu 50-146, Kaunas, LT-51368, Lithuania
[b] Institute of Cardiology, Lithuanian University of Health Sciences, Sukileliu Av. 17, Kaunas, LT-50009, Lithuania

A B S T R A C T

A theoretical framework describing the dynamics of nonlinear iterative maps of matrices is derived in this paper. It is shown that an iterative map of matrices does exhibit the effect of exponential divergence if the following two conditions are satisfied simultaneously. The first condition is that at least one of the multiplicity indexes of the eigenvalues of the matrix of initial conditions must be greater than one. The second condition is that the Lyapunov exponent of the corresponding scalar iterative map is greater than zero. The concept of packing and divergence codes is introduced to characterize the rate of the divergence of nonlinear iterative maps of matrices. Theoretical derivations and computational simulations yield counterintuitive results that the divergence rate of the logistic map of matrices is the same as of the circle map of matrices – even though the higher-order derivatives of the circle mapping function do not vanish.

1. Introduction

Most of the dynamics displayed by highly complicated nonlinear systems also appear for simple nonlinear systems [1]. A paradigmatic example of a simple discrete iterative system with very complicated dynamics is the logistic map introduced more than 40 years ago [2]. Discrete-time map-based models of networks comprising many units with global couplings have a long tradition in the physics of complex systems [3]. Coupled map lattices are spatially extended networks of dynamically interacting simple systems with a global or local coupling and the corresponding coupling terms [4]. Collective chaotic behavior of such coupled map lattices continues to attract attention from diverse fields of science and engineering [5–7].

However, the complexity of the system's architecture can be expanded not only by adding new elements in a coupled lattice of discrete iterative maps. It appears that the replacement of a discrete scalar variable by a square matrix of order 2 in a single iterative map can yield such counterintuitive phenomena like the explosive divergence [8]. The effect of the explosive divergence occurs when the Lyapunov exponent of the corresponding scalar iterative map becomes positive [9]. Complex transient processes (temporary divergence of a single iterative map of matrices of order 2, chimera states of spatiotemporal divergence in coupled maps of matrices of order 2) exist in the region of the onset of chaos of the corresponding scalar iterative map [10].

This transition space between bounded periodic orbits and the explosive divergence can be exploited for the construction of the image hiding scheme in a two-dimensional coupled lattice (where each node of the lattice is represented by the iterative map of matrices of order 2) [11]. The spatiotemporal divergence is employed to hide the secret digital image in the state map of the nodal variables of the lattice [11].

* Corresponding author.
E-mail address: minvydas.ragulskis@ktu.lt (M. Ragulskis).

As mentioned previously, the collective chaotic behavior of coupled map lattices remains an active area of research. Coupled lattices of iterative maps of matrices of order 2 can exhibit such new collective behavior as fractal-type spatiotemporal divergence [12]. One may expect that the effect of spatiotemporal divergence will become much more complex if the order of matrices becomes higher. Moreover, one may also expect that image hiding algorithms based on coupled lattices with higher-order matrices would be able to offer new functionality and security features. Clearly, all these potential applications cannot be constructed without building a solid theoretical foundation for a single uncoupled iterative map of matrices of order n.

The main objective of this paper is to investigate the dynamics of discrete iterative systems when a square matrix of order $n > 2$ replaces the discrete scalar variable. Such a replacement poses serious theoretical and computational challenges and provides an insight into the complex dynamics of discrete iterative systems of matrices. The ability to generalize the theory of iterative maps of square matrices when the order $n > 2$ would allow us to understand the behavior of such discrete nonlinear systems – especially in the transition state between order and chaos.

The concept of the packing and divergence codes is introduced in this paper. Packing codes are used to define algebraic multiplicities of matrix eigenvalues. Packing codes do represent the combinatorial bin packing problem [13]. In its turn, the combinatorial bin packing problem is related to the partition problem of a non-negative integer in number theory [14]. It appears that bins in a partition define the divergence properties of an iterative map of matrices. The newly introduced divergence codes represent relationships between the packing codes and divergence rates.

The paper is structured as follows. A short overview of the dynamics of iterative maps of square matrices of order two is given in Section 2. The packing codes and divergence codes are introduced in Section 3. Properties of the packing and divergence codes are discussed in Section 4. The divergence rate of iterative maps of matrices is assessed in Section 5. Computational experiments with the logistic map of matrices and the circle map of matrices are discussed in Section 6. Concluding remarks are given in the final section.

2. Preliminaries

This section gives a short overview of discrete iterative maps of matrices, where a discrete scalar variable is replaced by a square matrix of order 2 [8,9]. Let us consider a discrete iterative map:

$$x^{(k+1)} = f\left(x^{(k)}\right) \tag{1}$$

where $k = 0, 1, 2, \ldots$; f is the mapping function and $x^{(0)} \in \mathbb{R}$ is the initial condition. It is demonstrated in [9] that the scalar variable $x^{(k)}$ can be replaced by a matrix of variables $\mathbf{X}^{(k)} = \begin{bmatrix} x_{11}^{(k)} & x_{12}^{(k)} \\ x_{21}^{(k)} & x_{22}^{(k)} \end{bmatrix}$ if the scalar mapping function f is an algebraic function expandable into a power series

$$f(z) = \sum_{j=0}^{\infty} c_j \frac{z^j}{j!}; \tag{2}$$

where $z \in \mathbb{R}$; $x_{11}^{(k)}$, $x_{12}^{(k)}$, $x_{21}^{(k)}$, $x_{22}^{(k)} \in \mathbb{R}$; $c_j \in \mathbb{R}$; $\left|c_j\right| \le M < \infty$; $j = 0, 1, 2, \ldots$. It appears that the dynamics of such a discrete iterative map of matrices depends on the type of the matrix of initial conditions $\mathbf{X}^{(0)}$. If the eigenvalues of $\mathbf{X}^{(0)}$ are different ($\lambda_1^{(0)} \neq \lambda_2^{(0)}$), the matrix of initial conditions can be expressed in the form comprising a pair of conjugate idempotents [8]:

$$\mathbf{X}^{(0)} = \lambda_1^{(0)}\mathbf{D}_1 + \lambda_2^{(0)}\mathbf{D}_2 \tag{3}$$

where $\mathbf{D}_1 = \frac{1}{\lambda_1^{(0)} - \lambda_2^{(0)}}\left(\mathbf{X}^{(0)} - \lambda_2^{(0)}\mathbf{I}\right)$; $\mathbf{D}_2 = \frac{1}{\lambda_2^{(0)} - \lambda_1^{(0)}}\left(\mathbf{X}^{(0)} - \lambda_1^{(0)}\mathbf{I}\right)$ and $\mathbf{I}$ is the identity matrix. The following properties do hold for the pair of conjugate idempotents $\mathbf{D}_1$ and $\mathbf{D}_2$:

$$|\mathbf{D}_1| = |\mathbf{D}_2| = 0; \quad \mathbf{D}_1 + \mathbf{D}_2 = \mathbf{I}; \quad \mathbf{D}_1\mathbf{D}_1 = \mathbf{D}_1; \quad \mathbf{D}_2\mathbf{D}_2 = \mathbf{D}_2; \quad \mathbf{D}_1\mathbf{D}_2 = \mathbf{D}_2\mathbf{D}_1 = \begin{bmatrix} 0 & 0 \\ 0 & 0 \end{bmatrix}. \tag{4}$$

It appears that conjugate idempotents $\mathbf{D}_1$ and $\mathbf{D}_2$ remain unchanged as the iterative map of matrices evolves [9]:

$$\lambda_1^{(k+1)}\mathbf{D}_1 + \lambda_2^{(k+1)}\mathbf{D}_2 = f\left(\lambda_1^{(k)}\right)\mathbf{D}_1 + f\left(\lambda_2^{(k)}\right)\mathbf{D}_2; \quad k = 0, 1, 2, \ldots \tag{5}$$

In other words, the iterative map of matrices splits into two separate scalar maps:

$$\begin{cases} \lambda_1^{(k+1)} = f\left(\lambda_1^{(k)}\right); \\ \lambda_2^{(k+1)} = f\left(\lambda_2^{(k)}\right); \end{cases} \quad k = 0, 1, 2, \ldots \tag{6}$$

The situation changes completely if the two eigenvalues of $\mathbf{X}^{(0)}$ do coincide ($\lambda_1^{(0)} = \lambda_2^{(0)} = \lambda_0^{(0)}$). Then, the matrix of initial conditions can be expressed in a form of a nilpotent matrix [8]:

$$\mathbf{X}^{(0)} = \lambda_0^{(0)}\mathbf{I} + \mathbf{N}. \tag{7}$$

Table 1
Packing and divergence codes for the scalar iterative map. Packing codes show all different combinations of the multiplicity indexes of eigenvalues of the matrix of initial conditions. Divergence codes do represent the indexes of the parameter μ.

Code No.	Packing codes	Divergence codes
	Bin Size	1×1
	1	
1	1	0

The following properties do hold for the nilpotent $\mathbf{N}$ with index 2:

$$\mathbf{N}^2 = \begin{bmatrix} 0 & 0 \\ 0 & 0 \end{bmatrix}; \quad |\mathbf{N}| = 0. \tag{8}$$

Analogously, it appears that the nilpotent $\mathbf{N}$ remains unchanged as the iterative map of matrices evolves [9]:

$$\lambda_0^{(k+1)}\mathbf{I} + \mu_1^{(k+1)}\mathbf{N} = f\left(\lambda_0^{(k)}\right)\mathbf{I} + \mu_1^{(k)} f'\left(\lambda_0^{(k)}\right)\mathbf{N}; \quad k = 0, 1, 2, \ldots \tag{9}$$

where the derivative of the mapping function is computed according to Eq. (2): $f'(z) = \sum_{j=0}^{+\infty} c_{j+1} \frac{z^j}{j!}$.

In other words, the iterative map of matrices splits into two separate scalar maps:

$$\begin{cases} \lambda_0^{(k+1)} = f\left(\lambda_0^{(k)}\right); \\ \mu_1^{(k+1)} = \mu_1^{(k)} f'\left(\lambda_0^{(k)}\right); \end{cases} \quad k = 0, 1, 2, \ldots \tag{10}$$

where $\mu_1^{(0)} = 1$. The effect of explosive divergence may occur in the iterative map of matrices if the Lyapunov exponent of the scalar iterative map is positive [9]. This is a nonlinear phenomenon which is not observable in scalar iterative maps. As mentioned in the Introduction, the main objective of this paper is to explore similar effects of divergence when the dimension of the matrix variable is larger than 2.

3. Packing codes and divergence codes

The fact that the type of the matrix of initial conditions does pre-determine the evolution of iterative maps of matrices enables the construction of intuitive diagrams describing the divergence of these maps. The concept of the packing and divergence codes is introduced in this Section.

3.1. The iterative scalar map

Let us consider a scalar iterative map (the dimension of the matrix of the initial conditions is 1×1 (Table 1)). The scalar initial condition coincides with its eigenvalue $\lambda_0^{(0)}$ (the multiplicity of the eigenvalue is 1) – and the iterative map is described by a simple iterative equation

$$\lambda_0^{(k+1)} = f\left(\lambda_0^{(k)}\right), \quad k = 0, 1, 2, \ldots \tag{11}$$

Let us define the set of packing codes as the set of vectors of all possible combinations of multiplicity indexes of eigenvalues of the matrix of the initial conditions. The multiplicity index of a single eigenvalue is 1. Therefore the scalar iterative map does possess a single packing code equal to one (Table 1).

Let us define the set of divergence codes as a set of vectors describing the indexes of parameters μ (Eq. (10)). The scalar iterative map cannot comprise any nilpotents – the only scalar variable is $\lambda_0^{(k)}$ (Eq. (11)). Therefore, the divergence code for the scalar iterative map is zero (Table 1).

3.2. The iterative map of matrices of order 2

Without loss of generality, let us assume that the pair of conjugate idempotents and the nilpotent read:

$$\mathbf{D}_1 = \mathbf{T}\begin{bmatrix} 1 & 0 \\ 0 & 0 \end{bmatrix}\mathbf{T}^{-1}; \quad \mathbf{D}_2 = \mathbf{T}\begin{bmatrix} 0 & 0 \\ 0 & 1 \end{bmatrix}\mathbf{T}^{-1}; \quad \mathbf{N}_{12} = \mathbf{T}\begin{bmatrix} 0 & 1 \\ 0 & 0 \end{bmatrix}\mathbf{T}^{-1} \tag{12}$$

Table 2
The multiplication table between the second-order conjugate idempotents and the nilpotent $\mathbf{N}_{12}$.

$\cdot$	$\mathbf{D}_1$	$\mathbf{D}_2$	$\mathbf{N}_{12}$
$\mathbf{D}_1$	$\mathbf{D}_1$	Θ	$\mathbf{N}_{12}$
$\mathbf{D}_2$	Θ	$\mathbf{D}_2$	Θ
$\mathbf{N}_{12}$	Θ	$\mathbf{N}_{12}$	Θ

Table 3
The iterative map of matrices of order 2 splits into two scalar iterative maps.

Multiplicity indexes of eigenvalues	Scalar iterative systems	Indexes of the parameter μ
$\lambda_1^{(0)} \neq \lambda_2^{(0)}$ $\mathbf{0} \times 2 + \mathbf{2} \times 1$	$\begin{cases} \lambda_1^{(k+1)} = f\left(\lambda_1^{(k)}\right); \\ \lambda_2^{(k+1)} = f\left(\lambda_2^{(k)}\right); \end{cases}$ (13) $k = 0, 1, 2, \ldots$	$\cancel{\mu^{(k)}} \to [0]$ $\cancel{\mu^{(k)}} \to [0]$
$\lambda_1^{(0)} = \lambda_2^{(0)} = \lambda_0^{(0)}$ $\mathbf{1} \times 2 + \mathbf{0} \times 1$	$\begin{cases} \lambda_0^{(k+1)} = f\left(\lambda_0^{(k)}\right); \\ \mu_1^{(k+1)} = \mu_1^{(k)} f'\left(\lambda_0^{(k)}\right); \end{cases}$ (14) $k = 0, 1, 2, \ldots; \mu_1^{(0)} = 1.$	$\cancel{\mu^{(k)}} \to [0]$ $\mu_1^{(k)} \to [1]$

Table 4
Packing and divergence codes, when the matrix order is $n = 2$. The gray shaded area corresponds to the subset of divergence codes generated by a scalar iterative map.

Code No.	Packing codes		Divergence codes	
	Bin Size		2×2	
	2	1		
1	0	2	0	0
2	1	0	0	1

where $\mathbf{T} \in \mathbb{R}^{2\times 2}$; $|\mathbf{T}| \neq 0$. The table of multiplication between second-order idempotents and the nilpotent $\mathbf{N}_{12}$ is depicted in Table 2.

As discussed in the previous section, the iterative map of matrices of order 2 splits into two scalar iterative systems (Table 3). The first row of Table 3 corresponds to the case when two eigenvalues of the matrix of initial conditions are different. Two different eigenvalues with the multiplicity index equal to 1 and no eigenvalues with the multiplicity index equal to 2 yield the packing code $\mathbf{0} \times 2 + \mathbf{2} \times 1$ (Table 3).

Both scalar iterative maps in Eq. (14) do not comprise the parameter $\mu_1^{(k)}$. Thus, the divergence code comprises two zeros (Table 3).

The packing code $\mathbf{1} \times 2 + \mathbf{0} \times 1$ corresponds to the case when both eigenvalues of the matrix of initial conditions do coincide (Table 3). The parameter $\mu_1^{(k)}$ is present in the second scalar iterative map. Therefore, the divergence code reads [0 1] (Table 3).

Finally, packing and divergence codes are collected into a separate table (Table 4). The gray shaded area in divergence codes in Table 4 corresponds to the subset of divergence codes generated by a single scalar iterative map (Table 1).

Table 5
The multiplication table between third-order conjugate idempotents and nilpotents.

$\cdot$	$\mathbf{D}_1$	$\mathbf{D}_2$	$\mathbf{D}_3$	$\mathbf{N}_{12}$	$\mathbf{N}_{13}$	$\mathbf{N}_{23}$
$\mathbf{D}_1$	$\mathbf{D}_1$	Θ	Θ	$\mathbf{N}_{12}$	$\mathbf{N}_{13}$	Θ
$\mathbf{D}_2$	Θ	$\mathbf{D}_2$	Θ	Θ	Θ	$\mathbf{N}_{23}$
$\mathbf{D}_3$	Θ	Θ	$\mathbf{D}_3$	Θ	Θ	Θ
$\mathbf{N}_{12}$	Θ	$\mathbf{N}_{12}$	Θ	Θ	Θ	$\mathbf{N}_{13}$
$\mathbf{N}_{23}$	Θ	Θ	$\mathbf{N}_{23}$	Θ	Θ	Θ
$\mathbf{N}_{13}$	Θ	Θ	$\mathbf{N}_{13}$	Θ	Θ	Θ

3.3. The iterative map of matrices of order 3

Without loss of generality, let us assume that idempotents and nilpotents read:

$$\mathbf{D}_1 = \mathbf{T}\begin{bmatrix}1&0&0\\0&0&0\\0&0&0\end{bmatrix}\mathbf{T}^{-1},\quad \mathbf{D}_2 = \mathbf{T}\begin{bmatrix}0&0&0\\0&1&0\\0&0&0\end{bmatrix}\mathbf{T}^{-1},\quad \mathbf{D}_3 = \mathbf{T}\begin{bmatrix}0&0&0\\0&0&0\\0&0&1\end{bmatrix}\mathbf{T}^{-1}, \tag{15}$$

$$\mathbf{N}_{12} = \mathbf{T}\begin{bmatrix}0&1&0\\0&0&0\\0&0&0\end{bmatrix}\mathbf{T}^{-1},\quad \mathbf{N}_{13} = \mathbf{T}\begin{bmatrix}0&0&1\\0&0&0\\0&0&0\end{bmatrix}\mathbf{T}^{-1},\quad \mathbf{N}_{23} = \mathbf{T}\begin{bmatrix}0&0&0\\0&0&1\\0&0&0\end{bmatrix}\mathbf{T}^{-1}, \tag{16}$$

where $\mathbf{T} \in \mathbb{R}^{3\times 3}$; $|\mathbf{T}| \neq 0$. The table of multiplication between third-order conjugate idempotents and nilpotents is depicted in Table 5.

Note that the following equations hold true: $(\mathbf{N}_{12}+\mathbf{N}_{23})^2 = \mathbf{N}_{13}$; $(\mathbf{N}_{12}+\mathbf{N}_{23})\cdot\mathbf{N}_{13} = \mathbf{N}_{13}\cdot(\mathbf{N}_{12}+\mathbf{N}_{23}) = \Theta$.

Let us consider that the matrix of initial conditions $\mathbf{X}^{(0)}$ is expressed as $\mathbf{X}^{(0)} = \lambda_0^{(0)}\mathbf{I} + \mathbf{N}_{12} + \mathbf{N}_{23} + \mathbf{N}_{13}$. Then

$$\left(\mathbf{X}^{(0)}\right)^m = \left(\lambda_0^{(0)}\right)^m\mathbf{I} + m\left(\lambda_0^{(0)}\right)^{m-1}\mu_1^{(0)}(\mathbf{N}_{12}+\mathbf{N}_{23}) + \left(m\left(\lambda_0^{(0)}\right)^{m-1}\mu_2^{(0)} + \frac{m(m-1)}{2}\left(\lambda_0^{(0)}\right)^{m-2}\left(\mu_1^{(0)}\right)^2\right)\mathbf{N}_{13}, \tag{17}$$

where $m = 0, 1, 2, \ldots$; $\mu_1^{(0)} = \mu_2^{(0)} = 1$. The proof of Eq. (17) follows from Table 5 and the trinomial expansion formula:

$$(a+b+c)^m = \sum_{\substack{i_1+i_2+i_3=m\\ i_1,i_2,i_3\in\mathbb{Z}_0}} \frac{m!}{i_1!i_2!i_3!}a^{i_1}b^{i_2}c^{i_3}. \tag{18}$$

Then the iterative map of matrices $\mathbf{X}^{(k+1)} = f\left(\mathbf{X}^{(k)}\right)$ reads:

$$\begin{aligned}\mathbf{X}^{(k+1)} &= \lambda_0^{(k+1)}\mathbf{I} + \mu_1^{(k+1)}(\mathbf{N}_{12}+\mathbf{N}_{23}) + \mu_2^{(k+1)}\mathbf{N}_{13}\\ &= f\left(\lambda_0^{(k)}\right)\mathbf{I} + \mu_1^{(k)}f'\left(\lambda_0^{(k)}\right)(\mathbf{N}_{12}+\mathbf{N}_{23}) + \left(\mu_2^{(k)}f'\left(\lambda_0^{(k)}\right) + \frac{\left(\mu_1^{(k)}\right)^2}{2!}f''\left(\lambda_0^{(k)}\right)\right)\mathbf{N}_{13},\end{aligned} \tag{19}$$

where $k = 0, 1, 2, \ldots$; $f''(z) = \sum_{j=0}^{+\infty} c_{j+2}\frac{z^j}{j!}$; $\mu_1^{(0)} = \mu_2^{(0)} = 1$. Equality (19) yields recurrent relationships depicted in (22) (Table 6). Recurrent relationships in Eq. (20) and Eq. (21) (Table 6) are derived analogously.

Packing and divergence codes at $n = 3$ are depicted in Table 7. Note that the set of packing codes $\left\{\mathbf{P}^{(n)}\right\}$ does represent the classical bin packing problem in 1D. Really, $\mathbf{3}\times 1 = \mathbf{1}\times 2 + \mathbf{1}\times 1 = \mathbf{1}\times 3 = 3$ (Table 7). Moreover, all packing codes are sorted in the lexicographic order.

The divergence codes do represent the dynamics of scalar iterative systems in Eq. (20), Eq. (21) and Eq. (22) respectively (Table 7). The packing code [0 1 1] results into the divergence code [0 0 1] because Eq. (21) comprises two ordinary scalar iterative maps and one scalar map with the iterative variable $\mu_1^{(k)}$ (Table 7).

Analogously, the packing code [1 0 0] results into one scalar ordinary iterative map, one scalar iterative map comprising the iterative variable $\mu_1^{(k)}$, and one scalar iterative map comprising iterative variables $\mu_1^{(k)}$ and $\mu_2^{(k)}$ (Eq. (22)). The corresponding divergence code represents the highest index of the iterative variable $\mu_j^{(k)}$ in each of the scalar iterative equations in Eq. (22): [0 1 2] (Table 7). The gray shaded area in Table 7 corresponds to the subset of divergence codes generated by the iterative map of matrices of order 2 (Table 4).

Table 6
Iterative map of matrices of order 3 splits into three scalar iterative maps.

Multiplicity indexes of eigenvalues	Scalar iterative systems	Indexes of the parameter μ
$\lambda_1^{(0)} \neq \lambda_2^{(0)} \neq \lambda_3^{(0)}$ $\mathbf{0}\times 3+\mathbf{0}\times 2+\mathbf{3}\times 1$	$\begin{cases} \lambda_1^{(k+1)} = f\left(\lambda_1^{(k)}\right); \\ \lambda_2^{(k+1)} = f\left(\lambda_2^{(k)}\right); \\ \lambda_3^{(k+1)} = f\left(\lambda_3^{(k)}\right); \end{cases}$ (20) $k = 0, 1, 2, \ldots$	$\cancel{\mu^{(k)}} \to [0]$ $\cancel{\mu^{(k)}} \to [0]$ $\cancel{\mu^{(k)}} \to [0]$
$\lambda_1^{(0)} = \lambda_2^{(0)} = \lambda_0^{(0)} \neq \lambda_3^{(0)}$ $\mathbf{0}\times 3+\mathbf{1}\times 2+\mathbf{1}\times 1$	$\begin{cases} \lambda_0^{(k+1)} = f\left(\lambda_0^{(k)}\right); \\ \lambda_3^{(k+1)} = f\left(\lambda_3^{(k)}\right); \\ \mu_1^{(k+1)} = \mu_1^{(k)} f'\left(\lambda_0^{(k)}\right); \end{cases}$ (21) $k = 0, 1, 2, \ldots; \mu_1^{(0)} = 1.$	$\cancel{\mu^{(k)}} \to [0]$ $\cancel{\mu^{(k)}} \to [0]$ $\mu^{(k)}_{1} \to [1]$
$\lambda_1^{(0)} = \lambda_2^{(0)} = \lambda_3^{(0)} = \lambda_0^{(0)}$ $\mathbf{1}\times 3+\mathbf{0}\times 2+\mathbf{0}\times 1$	$\begin{cases} \lambda_0^{(k+1)} = f\left(\lambda_0^{(k)}\right); \\ \mu_1^{(k+1)} = \mu_1^{(k)} f'\left(\lambda_0^{(k)}\right); \\ \mu_2^{(k+1)} = \mu_2^{(k)} f'\left(\lambda_0^{(k)}\right) + \frac{\left(\mu_1^{(k)}\right)^2}{2!} f''\left(\lambda_0^{(k)}\right); \end{cases}$ (22) $k = 0, 1, 2, \ldots; \mu_1^{(0)} = 1; \mu_2^{(0)} = 1.$	$\cancel{\mu^{(k)}} \to [0]$ $\mu^{(k)}_{1} \to [1]$ $\mu^{(k)}_{2} \to [2]$

Table 7
Packing and divergence codes, when the matrix order is $n = 3$. The gray shaded area corresponds to the subset of divergence codes generated by the iterative map of matrices of order 2.

Code No.	Packing codes			Divergence codes		
	Bin size			3×3		
	3	2	1			
1	0	0	3	0	0	0
2	0	1	1	0	0	1
3	1	0	0	0	1	2

3.4. Iterative maps of matrices of order 4, 5 and n

Without loss of generality, let us consider the following idempotents:

$$\mathbf{D}_1 = \mathbf{T}\begin{bmatrix} 1 & 0 & 0 & 0 \\ 0 & 0 & 0 & 0 \\ 0 & 0 & 0 & 0 \\ 0 & 0 & 0 & 0 \end{bmatrix}\mathbf{T}^{-1}, \quad \mathbf{D}_2 = \mathbf{T}\begin{bmatrix} 0 & 0 & 0 & 0 \\ 0 & 1 & 0 & 0 \\ 0 & 0 & 0 & 0 \\ 0 & 0 & 0 & 0 \end{bmatrix}\mathbf{T}^{-1},$$
$$\mathbf{D}_3 = \mathbf{T}\begin{bmatrix} 0 & 0 & 0 & 0 \\ 0 & 0 & 0 & 0 \\ 0 & 0 & 1 & 0 \\ 0 & 0 & 0 & 0 \end{bmatrix}\mathbf{T}^{-1}, \quad \mathbf{D}_4 = \mathbf{T}\begin{bmatrix} 0 & 0 & 0 & 0 \\ 0 & 0 & 0 & 0 \\ 0 & 0 & 0 & 0 \\ 0 & 0 & 0 & 1 \end{bmatrix}\mathbf{T}^{-1}, \tag{23}$$

Table 8
The multiplication table between fourth-order idempotents and nilpotents.

$\cdot$	$\mathbf{D}_1$	$\mathbf{D}_2$	$\mathbf{D}_3$	$\mathbf{D}_4$	$\mathbf{N}_{12}$	$\mathbf{N}_{13}$	$\mathbf{N}_{14}$	$\mathbf{N}_{23}$	$\mathbf{N}_{24}$	$\mathbf{N}_{34}$
$\mathbf{D}_1$	$\mathbf{D}_1$	Θ	Θ	Θ	$\mathbf{N}_{12}$	$\mathbf{N}_{13}$	$\mathbf{N}_{14}$	Θ	Θ	Θ
$\mathbf{D}_2$	Θ	$\mathbf{D}_2$	Θ	Θ	Θ	Θ	Θ	$\mathbf{N}_{23}$	$\mathbf{N}_{24}$	Θ
$\mathbf{D}_3$	Θ	Θ	$\mathbf{D}_3$	Θ	Θ	Θ	Θ	Θ	Θ	$\mathbf{N}_{34}$
$\mathbf{D}_4$	Θ	Θ	Θ	$\mathbf{D}_4$	Θ	Θ	Θ	Θ	Θ	Θ
$\mathbf{N}_{12}$	Θ	$\mathbf{N}_{12}$	Θ	Θ	Θ	Θ	Θ	$\mathbf{N}_{13}$	$\mathbf{N}_{14}$	Θ
$\mathbf{N}_{13}$	Θ	Θ	$\mathbf{N}_{13}$	Θ	Θ	Θ	Θ	Θ	Θ	$\mathbf{N}_{14}$
$\mathbf{N}_{14}$	Θ	Θ	Θ	$\mathbf{N}_{14}$	Θ	Θ	Θ	Θ	Θ	Θ
$\mathbf{N}_{23}$	Θ	Θ	$\mathbf{N}_{23}$	Θ	Θ	Θ	Θ	Θ	Θ	$\mathbf{N}_{24}$
$\mathbf{N}_{24}$	Θ	Θ	Θ	$\mathbf{N}_{24}$	Θ	Θ	Θ	Θ	Θ	Θ
$\mathbf{N}_{34}$	Θ	Θ	Θ	$\mathbf{N}_{34}$	Θ	Θ	Θ	Θ	Θ	Θ

and nilpotents:

$$\mathbf{N}_{12}=\mathbf{T}\begin{bmatrix}0&1&0&0\\0&0&0&0\\0&0&0&0\\0&0&0&0\end{bmatrix}\mathbf{T}^{-1},\quad \mathbf{N}_{13}=\mathbf{T}\begin{bmatrix}0&0&1&0\\0&0&0&0\\0&0&0&0\\0&0&0&0\end{bmatrix}\mathbf{T}^{-1},\quad \mathbf{N}_{14}=\mathbf{T}\begin{bmatrix}0&0&0&1\\0&0&0&0\\0&0&0&0\\0&0&0&0\end{bmatrix}\mathbf{T}^{-1},$$
$$\mathbf{N}_{23}=\mathbf{T}\begin{bmatrix}0&0&0&0\\0&0&1&0\\0&0&0&0\\0&0&0&0\end{bmatrix}\mathbf{T}^{-1},\quad \mathbf{N}_{24}=\mathbf{T}\begin{bmatrix}0&0&0&0\\0&0&0&1\\0&0&0&0\\0&0&0&0\end{bmatrix}\mathbf{T}^{-1},\quad \mathbf{N}_{34}=\mathbf{T}\begin{bmatrix}0&0&0&0\\0&0&0&0\\0&0&0&1\\0&0&0&0\end{bmatrix}\mathbf{T}^{-1}, \tag{24}$$

where $\mathbf{T}$ is a nonsingular square matrix of order 4. Now, the multiplication table is given in Table 8.

The algebraic structure of the iterative map of matrices $\mathbf{X}^{(k+1)}=f\left(\mathbf{X}^{(k)}\right)$ can be deduced using analogous techniques as in the previous subsection. Scalar iterative systems are depicted in Table 9; packing and divergence codes – in Table 10. Gray shaded areas in Table 10 correspond to the subset of divergence codes generated by the iterative map of matrices of order 3 (Table 7).

Analogous derivations yield packing and divergence codes for the iterative map of matrices of order 5 (Table 11).

Packing and divergence codes are not enumerated for the iterative map of matrices of order n. Instead, the system of scalar iterative maps is depicted for the case when all eigenvalues of the matrix of initial conditions are equal ($\lambda_1^{(0)}=\lambda_2^{(0)}=\ldots=\lambda_n^{(0)}=\lambda_0^{(0)}$):

$$\begin{cases}\lambda_0^{(k+1)}=f\left(\lambda_0^{(k)}\right);\\ \mu_1^{(k+1)}=\mu_1^{(k)}f'\left(\lambda_0^{(k)}\right);\\ \mu_2^{(k+1)}=\mu_2^{(k)}f'\left(\lambda_0^{(k)}\right)+\frac{\left(\mu_1^{(k)}\right)^2}{2!}f''\left(\lambda_0^{(k)}\right);\\ \mu_3^{(k+1)}=\mu_3^{(k)}f'\left(\lambda_0^{(k)}\right)+\frac{2\mu_1^{(k)}\mu_2^{(k)}}{2!}f''\left(\lambda_0^{(k)}\right)+\frac{\left(\mu_1^{(k)}\right)^3}{3!}f'''\left(\lambda_0^{(k)}\right);\\ \mu_4^{(k+1)}=\mu_4^{(k)}f'\left(\lambda_0^{(k)}\right)+\frac{2\mu_1^{(k)}\mu_3^{(k)}+\left(\mu_2^{(k)}\right)^2}{2!}f''\left(\lambda_0^{(k)}\right)+\frac{3\left(\mu_1^{(k)}\right)^2\mu_2^{(k)}}{3!}f'''\left(\lambda_0^{(k)}\right)+\frac{\left(\mu_1^{(k)}\right)^4}{4!}f^{iv}\left(\lambda_0^{(k)}\right);\\ \ldots\\ \mu_{n-1}^{(k+1)}=\mu_{n-1}^{(k)}f'\left(\lambda_0^{(k)}\right)+\frac{\sum_{i_1=1}^{n-2}\mu_{i_1}^{(k)}\mu_{n-1-i_1}^{(k)}}{2!}f''\left(\lambda_0^{(k)}\right)+\frac{\sum_{1\le i_1,i_2,i_3\le n-3}^{i_1+i_2+i_3=n-1}\mu_{i_1}^{(k)}\mu_{i_2}^{(k)}\mu_{i_3}^{(k)}}{3!}f'''\left(\lambda_0^{(k)}\right)+\cdots+\frac{\left(\mu_1^{(k)}\right)^{n-1}}{(n-1)!}f^{(n-1)}\left(\lambda_0^{(k)}\right);\end{cases} \tag{30}$$

where $k=0,1,2,\ldots$; $\mu_1^{(0)}=\mu_2^{(0)}=\ldots=\mu_{n-1}^{(0)}=1$ and $f^{(n-1)}$ denotes the $(n-1)^{\text{st}}$ derivative of the mapping function f.

4. Properties of packing and divergence codes

Let us denote the set of packing codes and the set of divergence codes for a n-dimensional matrix of initial conditions $\mathbf{X}^{(0)}$ as $\left\{\mathbf{P}^{(n)}\right\}$ and $\left\{\mathbf{D}^{(n)}\right\}$ correspondingly.

Table 9
The iterative map of matrices of order 4 splits into five scalar iterative maps.

Multiplicity indexes of eigenvalues	Scalar iterative systems	Indexes of the parameter μ
$\lambda_1^{(0)} \neq \lambda_2^{(0)} \neq \lambda_3^{(0)} \neq \lambda_4^{(0)}$ $\mathbf{0}\times 4+\mathbf{0}\times 3+\mathbf{0}\times 2+\mathbf{4}\times 1$	$\begin{cases} \lambda_1^{(k+1)} = f\left(\lambda_1^{(k)}\right); \\ \lambda_2^{(k+1)} = f\left(\lambda_2^{(k)}\right); \\ \lambda_3^{(k+1)} = f\left(\lambda_3^{(k)}\right); \\ \lambda_4^{(k+1)} = f\left(\lambda_4^{(k)}\right); \end{cases}$ (25) $k = 0, 1, 2, \ldots$	$\cancel{\mu^{(k)}} \to [0]$ $\cancel{\mu^{(k)}} \to [0]$ $\cancel{\mu^{(k)}} \to [0]$ $\cancel{\mu^{(k)}} \to [0]$
$\lambda_1^{(0)} = \lambda_2^{(0)} = \lambda_0^{(0)} \neq \lambda_3^{(0)} \neq \lambda_4^{(0)}$ $\mathbf{0}\times 4+\mathbf{0}\times 3+\mathbf{1}\times 2+\mathbf{2}\times 1$	$\begin{cases} \lambda_0^{(k+1)} = f\left(\lambda_0^{(k)}\right); \\ \lambda_3^{(k+1)} = f\left(\lambda_3^{(k)}\right); \\ \lambda_4^{(k+1)} = f\left(\lambda_4^{(k)}\right); \\ \mu_1^{(k+1)} = \mu_1^{(k)} f'\left(\lambda_0^{(k)}\right); \end{cases}$ (26) $k = 0, 1, 2, \ldots; \mu_1^{(0)} = 1.$	$\cancel{\mu^{(k)}} \to [0]$ $\cancel{\mu^{(k)}} \to [0]$ $\cancel{\mu^{(k)}} \to [0]$ $\mu^{(k)}_{1} \to [1]$
$\lambda_1^{(0)} = \lambda_2^{(0)}; \quad \lambda_3^{(0)} = \lambda_4^{(0)}$ $\mathbf{0}\times 4+\mathbf{0}\times 3+\mathbf{2}\times 2+\mathbf{0}\times 1$	$\begin{cases} \lambda_1^{(k+1)} = f\left(\lambda_1^{(k)}\right); \\ \lambda_3^{(k+1)} = f\left(\lambda_3^{(k)}\right); \\ \mu_1^{(k+1),1} = \mu_1^{(k),1} f'\left(\lambda_1^{(k)}\right); \\ \mu_1^{(k+1),3} = \mu_1^{(k),3} f'\left(\lambda_3^{(k)}\right); \end{cases}$ (27) $k = 0, 1, 2, \ldots; \mu_1^{(0),1} = 1; \mu_1^{(0),3} = 1.$	$\cancel{\mu^{(k)}} \to [0]$ $\cancel{\mu^{(k)}} \to [0]$ $\mu^{(k),1}_{1} \to [1]$ $\mu^{(k),3}_{1} \to [1]$
$\lambda_1^{(0)} = \lambda_2^{(0)} = \lambda_3^{(0)} = \lambda_0^{(0)} \neq \lambda_4^{(0)}$ $\mathbf{0}\times 4+\mathbf{1}\times 3+\mathbf{0}\times 2+\mathbf{1}\times 1$	$\begin{cases} \lambda_0^{(k+1)} = f\left(\lambda_0^{(k)}\right); \\ \lambda_4^{(k+1)} = f\left(\lambda_4^{(k)}\right); \\ \mu_1^{(k+1)} = \mu_1^{(k)} f'\left(\lambda_0^{(k)}\right); \\ \mu_2^{(k+1)} = \mu_2^{(k)} f'\left(\lambda_0^{(k)}\right) + \frac{\left(\mu_1^{(k)}\right)^2}{2!} f''\left(\lambda_0^{(k)}\right); \end{cases}$ (28) $k = 0, 1, 2, \ldots; \mu_1^{(0)} = 1; \mu_2^{(0)} = 1.$	$\cancel{\mu^{(k)}} \to [0]$ $\cancel{\mu^{(k)}} \to [0]$ $\mu^{(k)}_{1} \to [1]$ $\mu^{(k)}_{2} \to [2]$
$\lambda_1^{(0)} = \lambda_2^{(0)} = \lambda_3^{(0)} = \lambda_4^{(0)} = \lambda_0^{(0)}$ $\mathbf{1}\times 4+\mathbf{0}\times 3+\mathbf{0}\times 2+\mathbf{0}\times 1$	$\begin{cases} \lambda_0^{(k+1)} = f\left(\lambda_0^{(k)}\right); \\ \mu_1^{(k+1)} = \mu_1^{(k)} f'\left(\lambda_0^{(k)}\right); \\ \mu_2^{(k+1)} = \mu_2^{(k)} f'\left(\lambda_0^{(k)}\right) + \frac{\left(\mu_1^{(k)}\right)^2}{2!} f''\left(\lambda_0^{(k)}\right); \\ \mu_3^{(k+1)} = \mu_3^{(k)} f'\left(\lambda_0^{(k)}\right) + \frac{2\mu_1^{(k)}\mu_2^{(k)}}{2!} f''\left(\lambda_0^{(k)}\right) + \frac{\left(\mu_1^{(k)}\right)^3}{3!} f'''\left(\lambda_0^{(k)}\right); \end{cases}$ (29) $k = 0, 1, 2, \ldots; \mu_1^{(0)} = 1; \mu_2^{(0)} = 1; \mu_3^{(0)} = 1.$	$\cancel{\mu^{(k)}} \to [0]$ $\mu^{(k)}_{1} \to [1]$ $\mu^{(k)}_{2} \to [2]$ $\mu^{(k)}_{3} \to [3]$

Property 1. *The set $\left\{\mathbf{P}^{(n)}\right\}$ does represent the combinatorial bin packing problem [13]. Therefore, the cardinality of the set $\left\{\mathbf{P}^{(n)}\right\}$ is defined by the following formula:*

$$\left|\left\{\mathbf{P}^{(n)}\right\}\right| = \frac{\alpha^{(n)}(0)}{n!} \tag{31}$$

where $\alpha^{(n)}(z)$ denotes the nth derivative of generating function $\alpha(z) = \prod_{j=1}^{n} \frac{1}{1-z^j}$ (the cardinality of the set for different n is shown in Table 12).

Table 10
Packing and divergence codes, when the matrix order is $n = 4$. The gray shaded area corresponds to the subset of divergence codes generated by the iterative map of matrices of order 3.

Code No.	Packing codes				Divergence codes			
	Bin size				5×4			
	4	3	2	1				
1	0	0	0	4	0	0	0	0
2	0	0	1	2	0	0	0	1
3	0	0	2	0	0	0	1	1
4	0	1	0	1	0	0	1	2
5	1	0	0	0	0	1	2	3

Table 11
Packing and divergence codes, when the matrix order is $n = 5$. The gray shaded area corresponds to the subset of divergence codes generated by the iterative map of matrices of order 4.

Code No.	Packing codes					Divergence codes				
	Bin size					7×5				
	5	4	3	2	1					
1	0	0	0	0	5	0	0	0	0	0
2	0	0	0	1	3	0	0	0	0	1
3	0	0	0	2	1	0	0	0	1	1
4	0	0	1	0	2	0	0	0	1	2
5	0	0	1	1	0	0	0	1	1	2
6	0	1	0	0	1	0	0	1	2	3
7	1	0	0	0	0	0	1	2	3	4

Table 12
The cardinality of the set of packing codes $\left\{\mathbf{P}^{(n)}\right\}$ depends on the dimension of the matrix of initial conditions $\mathbf{X}^{(0)}$ and is governed by the bin packing problem (where bins correspond to the multiplicity indexes of the eigenvalues of $\mathbf{X}^{(0)}$).

n	1	2	3	4	5	6	7	8	9
$\left\lvert\left\{\mathbf{P}^{(n)}\right\}\right\rvert$	1	2	3	5	7	11	15	22	30

Let us denote the digits of a packing code and the corresponding divergence code of an n-dimensional matrix as depicted in Table 13.

Property 2. *The cardinality of the set of packing codes and the set of divergence codes is equal for a fixed dimension of a square matrix.*

$$\left\lvert\left\{\mathbf{P}^{(n)}\right\}\right\rvert = \left\lvert\left\{\mathbf{D}^{(n)}\right\}\right\rvert. \tag{32}$$

Table 13
A schematic representation of the ordered numbers of a packing code and the corresponding divergence code for a n-dimensional matrix of initial conditions. Index k denotes the number of the packing code; $k = 1, 2, \ldots, \left|\left\{\mathbf{P}^{(n)}\right\}\right|$; $p_{k,1}, p_{k,2}, \ldots, p_{k,n} \in \mathbb{N}_0$; $d_{k,1}, d_{k,2}, \ldots, d_{k,n} \in \mathbb{N}_0$.

Bin size	n	$\cdots$	2	1
Digits of a packing code	$p_{k,n}$	$\cdots$	$p_{k,2}$	$p_{k,1}$
Digits of the divergence code	$d_{k,n}$	$\cdots$	$d_{k,2}$	$d_{k,1}$

Property 3. *Every packing code does represent an exact bin packing to n:*

$$\sum_{j=1}^{n} j p_{k,j} = n; \quad k = 1, 2, \ldots, \left|\left\{\mathbf{P}^{(n)}\right\}\right|. \tag{33}$$

Property 4. *The structure of the divergence code is uniquely pre-determined by its packing code. The digits in the divergence code are generated according to the following rule:*

$$\begin{aligned}\{d_{k,n} \ \cdots \ d_{k,2} \ d_{k,1}\} = \{&p_{k,1} \times [0]\} \\ \cup\{&p_{k,2} \times [0 \ 1]\} \\ \cup\{&p_{k,3} \times [0 \ 1 \ 2]\} \\ \cup \ &\cdots \\ \cup\{&p_{k,n} \times [0 \ 1 \ \cdots \ (n-2) \ (n-1)]\}\end{aligned} \tag{34}$$

where digits $d_{k,n} \ \cdots \ d_{k,2} \ d_{k,1}$ are sorted in the ascending order after the union operation; $k = 1, 2, \ldots, \left|\left\{\mathbf{P}^{(n)}\right\}\right|$.

For example, the divergence code of the packing code [0 0 2 0] is $\{2 \times [0 \ 1]\} = [0 \ 1 \ 0 \ 1] \Rightarrow [0 \ 0 \ 1 \ 1]$. But the divergence code of the packing code [0 1 0 1] is $\{1 \times [0 \ 1 \ 2]\} \cup \{1 \times [0]\} = [0 \ 1 \ 2 \ 0] \Rightarrow [0 \ 0 \ 1 \ 2]$.

Property 5. *The smallest packing code in the set $\left\{\mathbf{P}^{(n)}\right\}$ is $[0 \ \cdots \ 0 \ n]$. The corresponding divergence code reads: $[0 \ \cdots \ 0 \ 0]$.*

Property 6. *The largest packing code in the set $\left\{\mathbf{P}^{(n)}\right\}$ is $[1 \ 0 \ \cdots \ 0 \ 0]$. The corresponding divergence code reads: $[0 \ 1 \ \cdots \ (n-2) \ (n-1)]$.*

Property 7. *The set of divergence codes generated by a lower dimensional matrix is a subset of the set of divergence codes generated by a higher dimensional matrix:*

$$\left\{\mathbf{D}^{(1)}\right\} \subset \left\{\mathbf{D}^{(2)}\right\} \subset \cdots \subset \left\{\mathbf{D}^{(k)}\right\} \subset \left\{\mathbf{D}^{(k+1)}\right\} \subset \cdots \tag{35}$$

Subsets corresponding to sets $\left\{\mathbf{D}^{(k-1)}\right\}$ are marked in grayscale for $k = 2, 3, \ldots, 5$ in Tables 4 to 11 accordingly.

Property 8. *All packing codes in $\left\{\mathbf{P}^{(n)}\right\}$ are sorted in the lexicographic order. However, the same does not hold true for $\left\{\mathbf{D}^{(n)}\right\}$.*

For example, packing codes [0 0 0 2 0 0] and [0 0 1 0 0 2] (both for the iterative map of matrices of order 6) are mapped into divergence codes [0 0 1 1 2 2] and [0 0 0 1 2 3] accordingly. However, $1122 > 123$.

5. The divergence rate of iterative maps of matrices

It is demonstrated in the previous sections that an iterative map of matrices does split into scalar identical iterative maps if all eigenvalues of the matrix of initial conditions are different. Each scalar iterative map does not diverge if the parameters of the map and each distinct eigenvalue do fit into the stability region of the iterative map.

Without loss of generality, we will further consider the largest divergence codes only, which does correspond to the situation when all eigenvalues of the matrix of initial conditions are identical.

5.1. The logistic map of matrices of order n

Let us consider the paradigmatic logistic map $x^{(k+1)} = ax^{(k)}\left(1 - x^{(k)}\right)$ [2] where $0 < a \le 4$ and $0 \le x^{(k)} \le 1$. The largest divergence code for the $n \times n$ matrix $[0\ 1\ 2\ \ldots\ (n-2)\ (n-1)]$ yields reduced iterative equations (Eq. (30)) because higher derivatives of the logistic mapping function do vanish:

$$\begin{cases} \lambda_0^{(k+1)} = a\lambda_0^{(k)}\left(1 - \lambda_0^{(k)}\right); \\ \mu_1^{(k+1)} = a\mu_1^{(k)}\left(1 - 2\lambda_0^{(k)}\right); \\ \mu_2^{(k+1)} = a\mu_2^{(k)}\left(1 - 2\lambda_0^{(k)}\right) - a\left(\mu_1^{(k)}\right)^2; \\ \mu_3^{(k+1)} = a\mu_3^{(k)}\left(1 - 2\lambda_0^{(k)}\right) - 2a\mu_1^{(k)}\mu_2^{(k)}; \\ \ldots \\ \mu_{n-1}^{(k+1)} = a\mu_{n-1}^{(k)}\left(1 - 2\lambda_0^{(k)}\right) - a\sum\limits_{i_1=1}^{n-2}\mu_{i_1}^{(k)}\mu_{n-1-i_1}^{(k)}; \end{cases} \tag{36}$$

where $\mu_1^{(0)} = \mu_2^{(0)} = \ldots = \mu_{n-1}^{(0)} = 1$.

Note that the numerical estimate of the Lyapunov exponent for the logistic map reads [15]:

$$L = \frac{1}{k}\sum_{s=0}^{k-1}\ln\left(a\left|1 - 2\lambda_0^{(s)}\right|\right). \tag{37}$$

Then,

$$\ln\left(\left|\mu_1^{(k+1)}\right|\right) = \ln\left(\prod_{s=0}^{k}\left|f'\left(\lambda_0^{(s)}\right)\right|\right) = L(k+1). \tag{38}$$

Let us consider such a value of the parameter a that $L > 1$. Then, according to Eq. (38) the sequence $\left|\mu_1^{(k)}\right|$ will diverge exponentially. Such a divergence rate is linear – the growth of the elements of the sequence $\left|\mu_1^{(k)}\right|$ is comparable (in average) to the growth rate of a geometric progression with a common ratio L. The slope of a line describing the average growth of $\ln\left|\mu_1^{(k)}\right|$ is L (at large k).

This result helps to evaluate the growth rate of $\left|\mu_2^{(k)}\right|$. The term $\left|a\mu_2^{(k)}\left(1 - 2\lambda_0^{(k)}\right)\right|$ vanishes in respect of $\left|a\left(\mu_1^{(k)}\right)^2\right|$ at large k (note that $\mu_2^{(0)} = 1$). Then,

$$\lim_{k\to\infty}\ln\left|\mu_2^{(k)}\right| = \ln(a) + 2\ln\left|\mu_1^{(k)}\right| \tag{39}$$

In other words, the slope of a line approximating the average growth of $\ln\left|\mu_2^{(k)}\right|$ is $2L$ (at large k). Analogously,

$$\lim_{k\to\infty}\ln\left|\mu_3^{(k)}\right| = \ln(2a) + \ln\left|\mu_1^{(k)}\right| + \ln\left|\mu_2^{(k)}\right| \tag{40}$$

Therefore, the slope of a line approximating the average growth of $\ln\left|\mu_3^{(k)}\right|$ is $3L$.

Similarly, the growth rate of the terms $2\mu_1^{(k)}\mu_3^{(k)}$ and $\left(\mu_2^{(k)}\right)^2$ is comparable. Therefore, the slope of a line approximating the average growth of $\ln\left|\mu_4^{(k)}\right|$ is $4L$. Finally, the slope of a line approximating the average growth of $\ln\left|\mu_{n-1}^{(k)}\right|$ is $(n-1)L$.

5.2. The circle map of matrices of order n

The circle map is another paradigmatic model of a simple system exhibiting complex behavior [16]:

$$x^{(k+1)} = x^{(k)} + \Omega - \frac{K}{2\pi}\sin\left(2\pi x^{(k)}\right) \tag{41}$$

where $x^{(k)}$ is a normalized polar angle in the interval [0; 1]; K is the coupling strength and Ω is the driving phase. The principal difference between the circle map and the logistic map is that higher derivatives of the circle mapping function do not vanish. If all eigenvalues of the $n \times n$ matrix of initial conditions are equal, then the divergence code $[0\ 1\ 2\ \ldots\ (n-2)\ (n-1)]$ yields the following system of iterative equations:

$$\begin{cases} \lambda_0^{(k+1)} = \lambda_0^{(k)} + \Omega - \frac{K}{2\pi}\sin\left(2\pi\lambda_0^{(k)}\right); \\ \mu_1^{(k+1)} = \mu_1^{(k)}\left(1 - K\cos\left(2\pi\lambda_0^{(k)}\right)\right); \\ \mu_2^{(k+1)} = \mu_2^{(k)}\left(1 - K\cos\left(2\pi\lambda_0^{(k)}\right)\right) + \left(\mu_1^{(k)}\right)^2\pi K\sin\left(2\pi\lambda_0^{(k)}\right); \\ \mu_3^{(k+1)} = \mu_3^{(k)}\left(1 - K\cos\left(2\pi\lambda_0^{(k)}\right)\right) + 2\mu_1^{(k)}\mu_2^{(k)}\pi K\sin\left(2\pi\lambda_0^{(k)}\right) + \frac{2}{3}\left(\mu_1^{(k)}\right)^3\pi^2 K\cos\left(2\pi\lambda_0^{(k)}\right); \\ \ldots \\ \mu_{n-1}^{(k+1)} = \mu_{n-1}^{(k)}\left(1 - K\cos\left(2\pi\lambda_0^{(k)}\right)\right) + \cdots + \frac{\left(\mu_1^{(k)}\right)^{(n-1)}}{(n-1)!}(2\pi)^{n-2}K\sin\left(2\pi\lambda_0^{(k)} + \frac{(n-3)\pi}{2}\right); \end{cases} \tag{42}$$

where $\mu_1^{(0)} = \mu_2^{(0)} = \ldots = \mu_{n-1}^{(0)} = 1$.

Analogously, $\ln\left(\left|\mu_1^{(k+1)}\right|\right) = L(k+1)$, where L is the numerical estimate of the Lyapunov exponent for the circle map. The iterative equation for $\mu_2^{(k+1)}$ comprises two terms (Eq. (42)). But, again, the slope of a line approximating the average growth of $\ln\left|\mu_2^{(k)}\right|$ is $2L$ (at large k). However, the divergence rate of $\mu_3^{(k)}$ now comprises three terms (Eq. (42)). The first term $(\mu_3^{(k)}\left(1 - K\cos\left(2\pi\lambda_0^{(k)}\right)\right))$ vanishes in respect of the other two terms at large k. However, the growth rate of terms $\ln\left|\mu_1^{(k)}\mu_2^{(k)}\right|$ and $\ln\left|\left(\mu_1^{(k)}\right)^3\right|$ is the same ($L + 2L = 3L$). Therefore, the slope of a line approximating the average growth of $\ln\left|\mu_3^{(k)}\right|$ is $3L$ (at large k). The evaluation of the divergence rate of $\ln\left|\mu_{n-1}^{(k)}\right|$ requires more general analysis of the indexes of the parameter μ in the system of equations describing the dynamics of the iterative map of matrices (Eq. (30)).

The terms comprising the first derivatives of the mapping function yield the convergence rate which can be approximated by the Lyapunov exponent L (in the logarithmic frame). This fact is represented by the column of constants L at $f'(x)$ (Table 14).

The term at $f''(x)$ in the expression of $\mu_2^{(k+1)}$ comprises the product $\mu_1^{(k)}\mu_1^{(k)}$ (Eq. (30)). This fact is represented by indexes $1 \cdot 1$ in the appropriate cell in Table 14.

The term at $f''(x)$ in the expression of $\mu_3^{(k+1)}$ comprises the sum of products $\mu_1^{(k)}\mu_2^{(k)} + \mu_2^{(k)}\mu_1^{(k)}$. That is represented by indexes $1 \cdot 2 + 2 \cdot 1$ in Table 14. Analogously, the term at $f'''(x)$ in the expression of $\mu_3^{(k+1)}$ comprises the product $\mu_1^{(k)}\mu_1^{(k)}\mu_1^{(k)}$ – this is represented by indexes $1 \cdot 1 \cdot 1$ in Table 14.

Such symbolic interpretation of indexes (and appropriate divergence rates) up to $\mu_5^{(k)}$ is presented in Table 14. The rule of induction yields the following property.

Property 9. *The divergence rate of the scalar iterative maps in Eq. (30) is exponential. The slope of a line approximating the average growth of* $\ln\left|\mu_m^{(k)}\right|$ *is Lm (at large k) for* $m = 1, 2, \ldots, (n-1)$, *where L is the Lyapunov exponent of the scalar iterative map* $\lambda_0^{(k+1)} = f\left(\lambda_0^{(k)}\right)$.

Property 9 yields an unexpected and completely counter-intuitive result. The divergence rate of the logistic map of matrices is the same as the divergence rate of the circle map of matrices even though the higher derivatives of the circle map function do not vanish.

Table 14
Indexes of parameters μ in front of the derivatives of the mapping function in Eq. (30) define the appropriate divergence rates of the iterative map of matrices. The constant L is the Lyapunov exponent of the scalar map $\mu_m^{(k+1)} = \mu_m^{(k)} f'\left(\lambda_0^{(k)}\right)$; $\mu_m^{(0)} = 1$; $m = 1, 2, \ldots$. For example, the term in front of $f''\left(\lambda_0^{(k)}\right)$ in the expression of $\mu_4^{(k+1)}$ reads (Eq. (30)): $0.5\left(\mu_1^{(k)}\mu_3^{(k)} + \mu_2^{(k)}\mu_2^{(k)} + \mu_3^{(k)}\mu_1^{(k)}\right)$. Therefore, the indexes of μ in this term are marked as $1 \cdot 3 + 2 \cdot 2 + 3 \cdot 1$. The divergence rates of $\ln\left|\mu_1^{(k)}\right|$, $\ln\left|\mu_2^{(k)}\right|$, and $\ln\left|\mu_3^{(k)}\right|$ are L, $2L$, and $3L$. Therefore, the divergence rate of $\ln\left|\left(\mu_1^{(k)}\mu_3^{(k)} + 0.5\left(\mu_2^{(k)}\right)^2\right) f''\left(\lambda_0^{(k)}\right)\right|$ is not higher than $4L$.

	$f'(x)$	$f''(x)$		$f'''(x)$		$f^{iv}(x)$		$f^{v}(x)$	
$\mu_1^{(k+1)}$	L								
$\mu_2^{(k+1)}$	L	$1 \cdot 1$	$2L$						
$\mu_3^{(k+1)}$	L	$1 \cdot 2 + 2 \cdot 1$	$3L$	$1 \cdot 1 \cdot 1$	$3L$				
$\mu_4^{(k+1)}$	L	$1 \cdot 3 + 2 \cdot 2$ $+ 3 \cdot 1$	$4L$	$1 \cdot 1 \cdot 2 + 1 \cdot 2 \cdot 1$ $+ 2 \cdot 1 \cdot 1$	$4L$	$1 \cdot 1 \cdot 1 \cdot 1$	$4L$		
$\mu_5^{(k+1)}$	L	$1 \cdot 4 + 2 \cdot 3$ $+ 3 \cdot 2 + 4 \cdot 1$	$5L$	$1 \cdot 1 \cdot 3 + 1 \cdot 2 \cdot 2$ $+ 1 \cdot 3 \cdot 1 + 2 \cdot 1 \cdot 2$ $+ 2 \cdot 2 \cdot 1 + 3 \cdot 1 \cdot 1$	$5L$	$1 \cdot 1 \cdot 1 \cdot 2 + 1 \cdot 1 \cdot 2 \cdot 1$ $+ 1 \cdot 2 \cdot 1 \cdot 1 + 2 \cdot 1 \cdot 1 \cdot 1$	$5L$	$1 \cdot 1 \cdot 1 \cdot 1 \cdot 1$	$5L$

Finally, it must be noted that Table 14 is constructed for the largest divergence code (when all eigenvalues of the matrix of initial conditions do coincide). Analogous divergence tables can be constructed for any other divergence code and can provide an insight into the complex dynamics of iterative maps of matrices.

6. Computational experiments

6.1. The logistic map of matrices of order 4

Let us consider the logistic map of matrices of order 4 with the matrix of initial conditions

$$\mathbf{X}^{(0)} = T \begin{bmatrix} 0.1 & 1 & 1 & 1 \\ 0 & 0.1 & 1 & 1 \\ 0 & 0 & 0.1 & 1 \\ 0 & 0 & 0 & 0.1 \end{bmatrix} T^{-1}; \quad T = \begin{bmatrix} 1.2 & 1.8 & 0.2 & 1.3 \\ 1.5 & 1.8 & 0.9 & 0.6 \\ 0.6 & 0.3 & 0.1 & 1.4 \\ 1.1 & 0.5 & 1 & 1.2 \end{bmatrix}. \tag{43}$$

All eigenvalues of $\mathbf{X}^{(0)}$ do coincide (the multiplicity index of $\lambda_0^{(0)} = 0.1$ is 4). The divergence code [0 1 2 3] yields three different rates of divergence.

The bifurcation diagram of $\lambda_0^{(k)}$ in respect of the parameter a (Eq. (36)) is depicted in Fig. 1(a). Note that the a-axis in Fig. 1 is logarithmic in order to expand the region where the scalar logistic map exhibits chaotic behavior. The variation of the Lyapunov exponent of the scalar logistic map of $\lambda_0^{(k)}$ in respect of the parameter a is shown in Fig. 1(b).

Finally, the variation of $\mu_1^{(k)}$, $\mu_2^{(k)}$ and $\mu_3^{(k)}$ (Eq. (36)) in respect of the parameter a is shown in Fig. 1(c)–(e) respectively. Note that the bifurcation diagram of $\lambda_0^{(k)}$ is constructed by omitting the initial transient processes. First 500 iterations of $\lambda_0^{(k)}$ are dropped out before plotting the diagram. The situation is different with the plots of $\mu_1^{(k)}$, $\mu_2^{(k)}$ and $\mu_3^{(k)}$ because these parameters do diverge at larger values of a. Therefore, instead of dropping out, we plot the first 2000 iterations of $\mu_1^{(k)}$, $\mu_2^{(k)}$ and $\mu_3^{(k)}$.

Results of computational experiments in Fig. 1 confirm that $\mu_1^{(k)}$, $\mu_2^{(k)}$ and $\mu_3^{(k)}$ diverge when the Lyapunov exponent of the scalar logistic map is positive. The numerical values of $\left|\mu_1^{(k)}\right|$, $\left|\mu_1^{(k)}\right|$ and $\left|\mu_1^{(k)}\right|$ exceed 100 in several iterations at such a where the Lyapunov exponent is positive (Fig. 1(c)–(e)). Instead, the effect of transient oscillation [12] is observed at such values of a where the Lyapunov exponent is negative (Fig. 1(c)–(e)). The largest amplitudes of transient oscillations are observed at the period-2, period-4, period-8 bifurcation points (where the Lyapunov exponent is equal to zero). After some transient oscillation, $\mu_1^{(k)}$, $\mu_2^{(k)}$ and $\mu_3^{(k)}$ finally converge to zero when the Lyapunov exponent is negative (Fig. 1(c)–(e)).

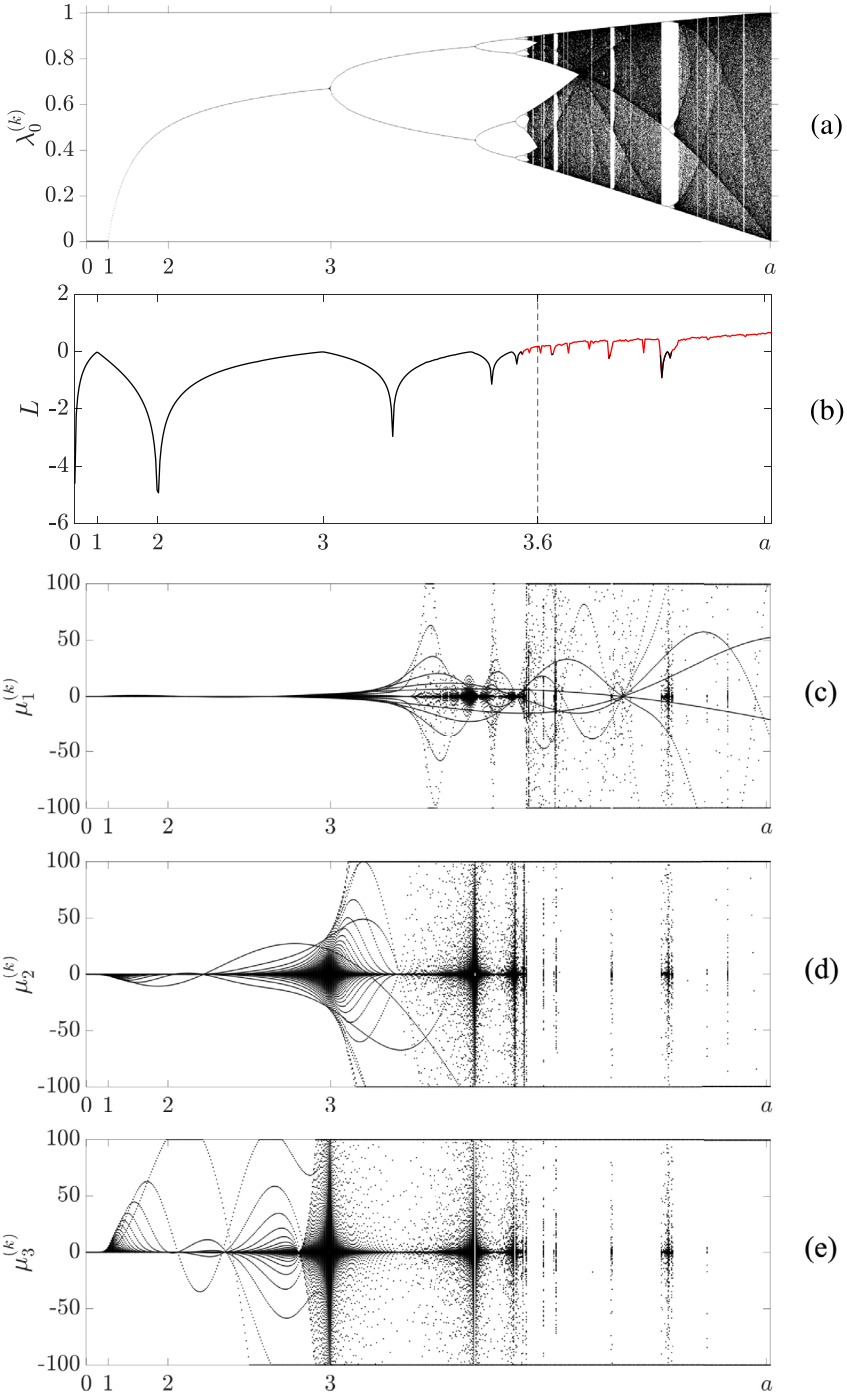

Fig. 1. The largest divergence code [0 1 2 3] yields three different divergence rates of the logistic map of matrices of order 4. The matrix of initial conditions is set as a nilpotent matrix $\mathbf{X}^{(0)} = T \begin{bmatrix} 0.1 & 1 & 1 & 1 \\ 0 & 0.1 & 1 & 1 \\ 0 & 0 & 0.1 & 1 \\ 0 & 0 & 0 & 0.1 \end{bmatrix} T^{-1}$; $T = \begin{bmatrix} 1.2 & 1.8 & 0.2 & 1.3 \\ 1.5 & 1.8 & 0.9 & 0.6 \\ 0.6 & 0.3 & 0.1 & 1.4 \\ 1.1 & 0.5 & 1 & 1.2 \end{bmatrix}$. The packing code of $\mathbf{X}^{(0)}$ is [1 0 0 0] because all four eigenvalues $\lambda_0^{(0)} = 0.1$ do coincide. The bifurcation diagram of the scalar logistic map $\lambda_0^{(k+1)} = a\lambda_0^{(k)}\left(1 - \lambda_0^{(k)}\right)$ is shown in part (a). The Lyapunov exponent computed for the scalar logistic map is depicted in part (b) (values greater than zero are marked in red). The evolution of parameters $\mu_1^{(k)}$, $\mu_2^{(k)}$, and $\mu_3^{(k)}$; $k = 0, 1, 2, \ldots$ is shown in parts (c), (d), and (e). The explosive divergence of $\mu_1^{(k)}$, $\mu_2^{(k)}$, and $\mu_3^{(k)}$ is observed when the Lyapunov exponent of the scalar logistic map is positive. The vertical dashed line in part (b) denotes the value of parameter a used to explore the rate of divergence of $\mu_1^{(k)}$, $\mu_2^{(k)}$, and $\mu_3^{(k)}$ in Fig. 2.

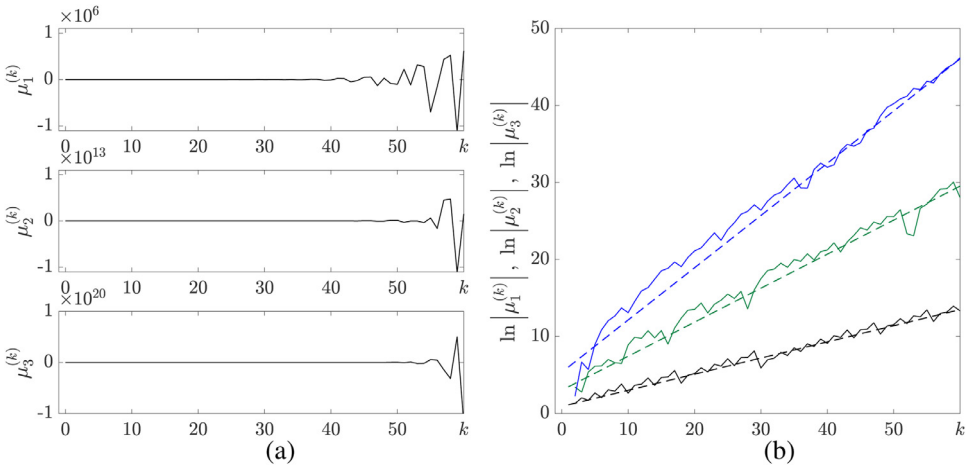

Fig. 2. The explosive divergence rate of the logistic map of matrices of order 4 is determined by the Lyapunov exponent of the scalar logistic map. The matrix of initial conditions is set as a nilpotent matrix $\mathbf{X}^{(0)} = T \begin{bmatrix} 0.1 & 1 & 1 & 1 \\ 0 & 0.1 & 1 & 1 \\ 0 & 0 & 0.1 & 1 \\ 0 & 0 & 0 & 0.1 \end{bmatrix} T^{-1}$; $T = \begin{bmatrix} 1.2 & 1.8 & 0.2 & 1.3 \\ 1.5 & 1.8 & 0.9 & 0.6 \\ 0.6 & 0.3 & 0.1 & 1.4 \\ 1.1 & 0.5 & 1 & 1.2 \end{bmatrix}$. The parameter of the logistic map a is set to 3.6. The Lyapunov exponent L of the scalar logistic map at $a = 3.6$ is 0.197. The evolution of $\mu_1^{(k)}$, $\mu_2^{(k)}$, and $\mu_3^{(k)}$ is shown in part (a). The evolution of $\ln\left|\mu_1^{(k)}\right|$, $\ln\left|\mu_2^{(k)}\right|$, and $\ln\left|\mu_3^{(k)}\right|$ is represented by the black line, the green line, and the blue line respectively in part (b). The growth of $\ln\left|\mu_1^{(k)}\right|$ is approximated by the black dashed line with the slope coefficient equal to $0.21 \approx L$. The growth of $\ln\left|\mu_2^{(k)}\right|$ is approximated by the green dashed line with the slope coefficient equal to $0.442 \approx 2L$. The growth of $\ln\left|\mu_3^{(k)}\right|$ is approximated by the blue dashed line with the slope coefficient equal to $0.679 \approx 3L$.

The divergence rate of the logistic map of matrices of order 4 is further investigated at $a = 3.6$. The first 60 iterations of $\mu_1^{(k)}$, $\mu_2^{(k)}$ and $\mu_3^{(k)}$ are depicted in Fig. 2(a) (note that the scale of the vertical axis is different in all three subgraphs). The same 60 iterations – but of $\ln\left|\mu_1^{(k)}\right|$, $\ln\left|\mu_2^{(k)}\right|$, and $\ln\left|\mu_3^{(k)}\right|$ are shown in solid lines in Fig. 2(b). Linear approximation of the evolution of $\ln\left|\mu_1^{(k)}\right|$, $\ln\left|\mu_2^{(k)}\right|$, and $\ln\left|\mu_3^{(k)}\right|$ yields regression lines $y = 0.210x + 0.911$, $y = 0.442x + 3.014$, and $y = 0.679x + 5.353$ represented as dashed lines in Fig. 2(b). The ratio between the slope coefficients of these lines read: $\frac{0.442}{0.210} = 2.105$ and $\frac{0.679}{0.210} = 3.233$.

This result does comply very well with the formal assessment of the divergence rates in Table 14. Note that the computations are performed right from the initial conditions without dropping initial transients and letting the iteration number tend to plus infinity.

6.2. The circle map of matrices of order 4

Computational experiments are continued with the circle map of matrices of order 4 with the same matrix of initial conditions as used for the logistic map (Eq. (43)). The parameter Ω is fixed to 0.15; the parameter K is varied from 1 to 3.4 (Fig. 3).

The bifurcation diagram of $\lambda_0^{(k)}$ in respect of the parameter K is shown in Fig. 3(a). The variation of the Lyapunov exponent of the scalar circle map of $\lambda_0^{(k)}$ in respect of the parameter K is depicted in Fig. 3(b). The variation of $\mu_1^{(k)}$, $\mu_2^{(k)}$ and $\mu_3^{(k)}$ in respect of the parameter K is shown in Fig. 3(c)–(e) respectively.

The divergence rate of the circle map of matrices of order 4 is further investigated at $K = 3$. The first 60 iterations of $\mu_1^{(k)}$, $\mu_2^{(k)}$, and $\mu_3^{(k)}$ are shown in Fig. 4(a). Initial iterations of $\ln\left|\mu_1^{(k)}\right|$, $\ln\left|\mu_2^{(k)}\right|$, and $\ln\left|\mu_3^{(k)}\right|$ are depicted as solid lines in Fig. 4(b). Linear approximation of these lines yield regression lines $y = 0.316x - 0.203$, $y = 0.678x + 0.865$, and $y = 1.018x + 1.946$ represented as dashed lines in Fig. 4(b). The ratio between the slope coefficients of these lines read: $\frac{0.678}{0.316} = 2.146$ and $\frac{1.018}{0.316} = 3.222$.

This result again shows a very good correspondence to the divergence rates derived in Table 14. Again, the computations are performed right from the initial conditions without letting the iteration number tend to plus infinity.

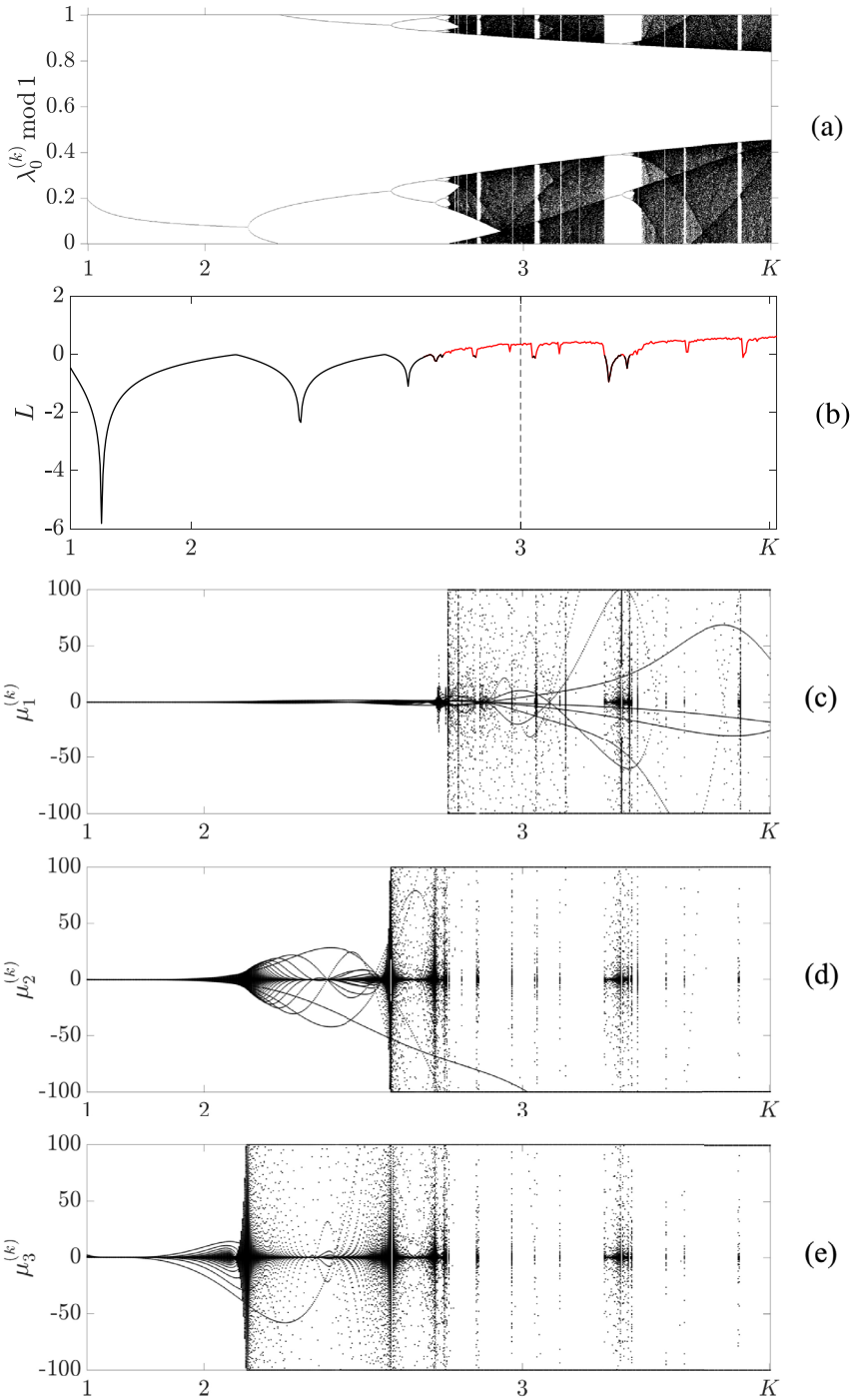

Fig. 3. The largest divergence code [0 1 2 3] yields three different divergence rates of the circle map of matrices of order 4. The matrix of initial conditions is set as a nilpotent matrix $\mathbf{X}^{(0)} = T \begin{bmatrix} 0.1 & 1 & 1 & 1 \\ 0 & 0.1 & 1 & 1 \\ 0 & 0 & 0.1 & 1 \\ 0 & 0 & 0 & 0.1 \end{bmatrix} T^{-1}$; $T = \begin{bmatrix} 1.2 & 1.8 & 0.2 & 1.3 \\ 1.5 & 1.8 & 0.9 & 0.6 \\ 0.6 & 0.3 & 0.1 & 1.4 \\ 1.1 & 0.5 & 1 & 1.2 \end{bmatrix}$. The packing code of $\mathbf{X}^{(0)}$ is [1 0 0 0] because all four eigenvalues $\lambda_0^{(0)} = 0.1$ do coincide. The bifurcation diagram of the scalar circle map $\lambda_0^{(k+1)} = \lambda_0^{(k)} + \Omega - \frac{K}{2\pi} \sin\left(2\pi\lambda_0^{(k)}\right)$ is shown in part (a) (parameter Ω is fixed to 0.15). The Lyapunov exponent computed for the scalar circle map is depicted in part (b) (values greater than zero are marked in red). The evolution of parameters $\mu_1^{(k)}$, $\mu_2^{(k)}$, and $\mu_3^{(k)}$; $k = 0, 1, 2, \ldots$ is shown in parts (c), (d), and (e). The explosive divergence of $\mu_1^{(k)}$, $\mu_2^{(k)}$, and $\mu_3^{(k)}$ is observed when the Lyapunov exponent of the scalar circle map is positive. The vertical dashed line in part (b) denotes the value of parameter K used to explore the rate of divergence of $\mu_1^{(k)}$, $\mu_2^{(k)}$, and $\mu_3^{(k)}$ in Fig. 4.

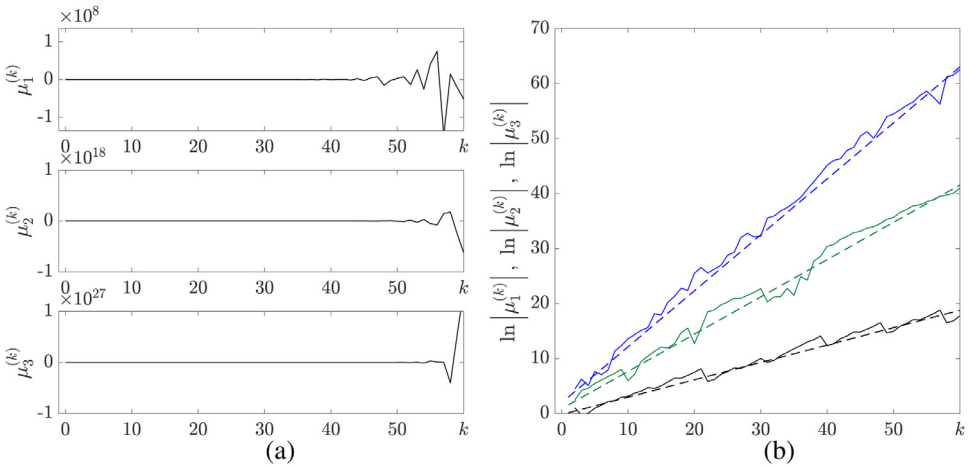

Fig. 4. The divergence rate of the circle map of matrices of order 4 is comparable to the divergence rate of the logistic map of matrices of order 4. This is a counterintuitive result because higher derivatives of the circle mapping function do not vanish (contrary to the logistic mapping function). The matrix of initial conditions is set as a nilpotent matrix $\mathbf{X}^{(0)} = T \begin{bmatrix} 0.1 & 1 & 1 & 1 \\ 0 & 0.1 & 1 & 1 \\ 0 & 0 & 0.1 & 1 \\ 0 & 0 & 0 & 0.1 \end{bmatrix} T^{-1}$; $T = \begin{bmatrix} 1.2 & 1.8 & 0.2 & 1.3 \\ 1.5 & 1.8 & 0.9 & 0.6 \\ 0.6 & 0.3 & 0.1 & 1.4 \\ 1.1 & 0.5 & 1 & 1.2 \end{bmatrix}$. The parameters of the circle map are set to $K = 3$; $\Omega = 0.15$. The Lyapunov exponent L of the scalar circle map is 0.331 at $K = 3$; $\Omega = 0.15$. The evolution of $\mu_1^{(k)}$, $\mu_2^{(k)}$, and $\mu_3^{(k)}$ is shown in part (a). The evolution of $\ln\left|\mu_1^{(k)}\right|$, $\ln\left|\mu_2^{(k)}\right|$, and $\ln\left|\mu_3^{(k)}\right|$ is represented by the black line, the green line, and the blue line respectively in part (b). The growth of $\ln\left|\mu_1^{(k)}\right|$ is approximated by the black dashed line with the slope coefficient equal to $0.316 \approx L$. The growth of $\ln\left|\mu_2^{(k)}\right|$ is approximated by the green dashed line with the slope coefficient equal to $0.678 \approx 2L$. The growth of $\ln\left|\mu_3^{(k)}\right|$ is approximated by the blue dashed line with the slope coefficient equal to $1.018 \approx 3L$.

7. Concluding remarks

The divergence of iterative maps of matrices is studied in this paper. The divergence properties are illustrated using the logistic map of matrices and the circle map of matrices. The main reason for selecting those two particular maps is based on the fact that higher derivatives of the logistic map function do vanish. Still, higher derivatives of the circle map function are not equal to zero. The developed theory holds for any other types of iterative maps where the memory horizon is equal to a single time step.

It has been demonstrated in the previous studies that a coupled map lattice of iterative maps of matrices of order 2 can exhibit such complex nonlinear effects as chimera states of spatiotemporal divergence [12]. Moreover, it appears that transient oscillations in 2-dimensional coupled map lattices of matrices of order 2 can be exploited for the development of a new type of image hiding algorithms [11]. The concept of those image hiding algorithms is based on the level-set method [17]. Each node of the coupled lattice does represent an iterative map of matrices. Each iterative map yields a response function in time. The level set method is used to crop each node's response function when the lattice is brought into the diverging mode [12]. A subtle control of initial conditions helps to reconstruct the encrypted digital image in the cropped representation of the lattice's divergence [11].

The results of this paper build the foundation for designing such image hiding algorithms where several different images can be simultaneously encoded in different layers (corresponding to different rates of divergence in the same iterative map of matrices). The functionality of such an image hiding scheme (at a fixed pixel in spatial coordinates) can be illustrated using Fig. 4. Let us assume that the crop level is set to 10 (in the logarithmic scale). The blue line and the green line will exceed the pre-set level after 20 time-forward iterations (Fig. 4b), and the corresponding pixel will become highlighted. However, the black line will still stay below the crop level after 20 time-forward iterations (Fig. 4b), and the corresponding pixel will remain dark. A proper interplay between the three different crop levels and the number of time-forward steps would allow hiding three different images in a 2-dimensional coupled map lattice of matrices of order 4.

Such an approach promises a new security level for such an image hiding algorithm. The development of such algorithms, as well as the exploration of complex Chimera type effects [10] in 1-dimensional and 2-dimensional coupled map lattices of matrices of order higher than two, do remain a clear objective for future research.

Declaration of Competing Interest

The authors declare that they have no known competing financial interests or personal relationships that could have appeared to influence the work reported in this paper.

CRediT authorship contribution statement

Rasa Smidtaite: Software, Formal analysis, Visualization. **Zenonas Navickas:** Formal analysis, Validation. **Minvydas Ragulskis:** Conceptualization, Methodology, Writing - review & editing.

References

[1] Lynch S. Nonlinear discrete dynamical systems. Dynamical systems with applications using mathematica. Boston: Birkhäuser; 2007. doi:101007/978-0-8176-4586-1_13.
[2] May RM. Simple mathematical models with very complicated dynamics. Nature 1976;261:459–67. doi:10.1038/261459a0.
[3] Kaneko K. Theory and applications of coupled map lattices. New York, NY: Wiley; 1993.
[4] Gupte N, Sharma A, Pradhan GR. Dynamical and statistical behaviour of coupled map lattices. Physica A 2003;318(1–2):85–91. doi:10.1016/S0378-4371(02)01410-3.
[5] Zhang Y-Q, Wang XY. A new image encryption algorithm based on non-adjacent coupled map lattices. Appl Soft Comput 2015;26:10–20. doi:10.1016/j.asoc.2014.09.039.
[6] Nozawa E. Coupled map lattice for the spiral pattern formation in astronomical objects. Physica D 2020;405:132377. doi:10.1016/j.physd.2020.132377.
[7] Kumar S, Kumar R, Kumar S, Kumar S. Cryptographic construction using coupled map lattice as a diffusion model to enhanced security. J Inf Secur Appl 2019;46:70–83. doi:10.1016/j.jisa.2019.02.011.
[8] Navickas Z, Smidtaite R, Vainoras A, Ragulskis M. The logistic map of matrices. Discrete Cont Dyn-B 2011;16(3):927–44. doi:10.3934/dcdsb.2011.16.927.
[9] Navickas Z, Ragulskis M, Vainoras A, Smidtaite R. The explosive divergence in iterative maps of matrices. Commun Nonlinear Sci 2012;17(11):4430–8. doi:10.1016/j.cnsns.2012.03.018.
[10] Smidtaite R, Guangqing L, Ragulskis M. Image entropy for the identification of chimera states of spatiotemporal divergence in complex coupled maps of matrices. Entropy 2019;21(5):523. doi:10.3390/e21050523.
[11] Guangqing L, Smidtaite R, Howard D, Ragulskis M. An image hiding scheme in a 2-dimensional coupled map lattice of matrices. Chaos Solitons Fractals 2019;124:78–85. doi:10.1016/j.chaos.2019.04.038.
[12] Guangqing L, Smidtaite R, Navickas Z, Ragulskis M. The effect of explosive divergence in a coupled map lattice of matrices. Chaos Solitons Fractals 2018;113:308–13. doi:10.1016/j.chaos.2018.06.016.
[13] Guichard D. An introduction to combinatorics and graph theory. Open Educational Resource (OER); 2016. URL https://www.whitman.edu/mathematics/cgt_online/cgt.pdf
[14] Hardy GH, Wright EM. An introduction to the theory of numbers. 6th ed. Oxford University Press; 2008. [1938]
[15] Hilborn RC. Chaos and nonlinear dynamics: an introduction for scientists and engineers. Oxford University Press; 2000. doi:101093/acprof:oso/9780198507239001001.
[16] Glass L, Guevara MR, Shrier A, Perez R. Bifurcation and chaos in a periodically stimulated cardiac oscillator. Physica D 1983;7(1–3):89–101. doi:10.1016/0167-2789(83)90119-7.
[17] Osher SJ, Fedkiw RP. Level set methods and dynamic implicit surfaces. Springer-Verlag; 2002.